technical memorandum

Daresbury Laborato

DL/SCI/TM64E

STATION 9.5 - COMMISSIONING STAGE RESULTS. 1. UNFOCUSSED LAUE

by

J. HABASH and S. HARROP, University of Manchester;
J. HELLIWELL, University of Manchester and SERC Daresbury Laboratory; and
C. NAVE and A. THOMPSON, SERC Daresbury Laboratory

FEBRUARY, 1990

Science and Engineering Research Council
DARESBURY LABORATORY
Daresbury, Warrington WA4 4AD

Station 9.5 - Commissioning Stage Results.
1. Unfocussed Laue.

J. Habash*, S. Harrop*, J. Helliwell*+ C. Nave+ and A. Thompson+.

* University of Manchester, Dept of Chemistry.
+ SERC, Daresbury Laboratory.

Abstract.

Test data has been collected on station 9.5, using the unfocussed white beam, in order to assess the station's usefulness for collecting Laue diffraction data from both proteins and small molecules. It is shown that accurate data can be obtained over the wavelength range 0.2 - 2.0 Å, and that exposure times are roughly commensurate with those obtained on 9.7 (taking into account the expected factor of four reduction in intensity of 9.5 with respect to 9.7).

Variation in the contributions of the two poles of the superconducting wiggler to the intensity seen on station 9.5 has highlighted the requirement for efficient horizontal steering of the SRS.

1. Introduction.

The jointly funded Swedish/SERC station on the wiggler beam line of the Daresbury SRS (Brammer et al (1988)) has been commissioned in one of its operational modes (unfocussed Laue) and data collected from two crystal samples. This serves as a basis for the other modes of operation involving mirror and/or monochromator, and to evaluate its utility for the collection of good quality Laue data.

Data recorded on 9.6 have already provided interpretable protein heavy atom difference Patterson maps, for example Helliwell (1989), and Laue data on station 9.7 has led to a high quality crystal structure solution and refinement. Hence, a straightforward comparison of data quality from station 9.7 or 9.6 with that of 9.5 is a valid way of assessing 9.5's likely impact in structure determination. The crystal samples were chosen because they had been extensively studied on stations 9.6 and 9.7 in Laue mode, and are typical of the type of problem investigated using the Laue technique. These samples were a crystal of the protein concanavalin - A (called con - A in the text), and a small organic molecule (the "red" crystal in the text). The same crystal was used on each station with identical data collection protocols in the respective cases. For the red crystal work, the sample was the same one used to perform a comparison of Laue and monochromatic X - ray analyses (M. Helliwell et al,(1989)).

The optics associated with the other modes of operation of 9.5 (focussed Laue and rapidly tuneable monochromatic) will shortly be installed, and it is intended to complete the documentation of the station commissioning phase by similar test experiments in these modes. This will be reported in a later technical memorandum.

2. Station Parameters Tested.

The following tests were made on station 9.5 :

a) Overall intensity available on the station was determined by comparing exposure times and ion chamber readings (using the same ionisation chamber, collimator etc).

b) The wavelength normalisation functions (λ - curves) for 9.5 and 9.7 were compared by taking Laue diffraction patterns on both stations with the same sample.

Calculations of the composite spectral profile and from the two separated sources were also made along the lines of the work reported by Greaves et al (1983) using software developed by Laundy.

3. Experimental.

The experimental layout of station 9.5 is given in fig 1, and that of the front end of 9.7 in Clark (1988). Film packs from the red crystal were recorded on station 9.5 (SRS 2GeV, Wiggler 5T, 292mA), and on 9.7 (SRS 2GeV, Wiggler 5T, 281 mA) using the same sample, the same collimator and the same goniostat. Three film packs (6 films each) were exposed at spindle readings of 23°, 26° and 29° using a 0.2 mm collimator. Exposure times on 9.5 were 0.8s (ion chamber 0.9×10^{-8} A) and on 9.7, 0.1 s (4×10^{-8} A), the 9.5 patterns being stronger.

Similarly, data were collected from a con-A crystal at spindle angles of 35° and 125° (this time using different goniostats) exposing *different* sections of the *same* crystal (to avoid radiation damage) and during the *same* SRS injection. The 9.7 exposures were made first (exposure 0.75s, 300 mA), followed a short while later by 9.5 (exposure 3s, 252 mA). Some of the diffraction patterns recorded are presented in Figs 2 - 7.

Fig 8 shows the geometrical arrangement of stations 9.5 and 9.7 with respect to the SRS wiggler source. It can be seen that the two sources overlap closely for 9.7 due to the wide viewing angle, whereas for 9.5 they are well separated and may be expected to be resolved with a suitable pinhole arrangement in the hutch.

4. Data Processing and Results.

The red crystal films were processed using the suite of Laue software developed at Daresbury by Machin (1987) based on the procedures for analysing Laue photographs described in Helliwell (1985) and Helliwell et al (1989). The method of using symmetry equivalent reflections being recorded at different wavelengths, and the appropriate computer program LAUENORM (Campbell, Habash, Helliwell and Moffat (1986)), were used to determine the λ - curve for the instrument and sample. Hence the λ - curve for stations 9.5 and 9.7 were established, the red crystal data giving the curve to only 1.2 Å at the minimum crystal to film distance available on the Laue camera. The protein gives the curve to > 2 Å, but since the "A" film from the con - A crystal recorded on 9.7 was too strong to process, only the λ - curve from 9.5 for the protein case is presented. Visual inspection of the "A" film from the protein collected on 9.5 (fig 6) shows significant intensity for spots at the edge of the films (i.e stimulated mainly by the longer wavelengths).

The λ - curves are presented in fig 9, and should be compared with the ratios of flux on 9.5 and 9.7 (vertically integrated over 0.2mm) calculated using the program due to Laundy (unpublished). These calculations (table 1) show a significant contribution to the overall intensity (particularly at longer wavelengths) of the wiggler side pole to 9.7. Confirmation of the source separation, measured by a pinhole camera on 9.5, has been hampered by variability in the storage

ring horizontal orbit, the variation of which can be sufficient to occlude one of the two source on 9.5.

The experimental λ - curves show the expected bias towards harder radiation on station 9.5. This bias towards harder wavelengths, and the theoretically smaller post - collimator beam divergence, may make 9.5 particularly attractive for virus crystallography in its unfocussed mode.

Inspection of the intensities of the diffraction patterns show that the 9.5 red crystal "A" film (0.8s) is significantly stronger than the 9.7 (0.1s) film, thus roughly confirming the geometrical factor of four in intensity expected between the two stations. The protein case, however, shows the 9.7 "B" film to be of a more similar intensity to the 9.5 "A" film (exposures 0.75 and 3s respectively, beam currents 300mA and 250mA respectively). This is presumably due to the contribution of the second source to the 9.7 photograph, enhancing the intensity at longer wavelengths.

The R factors give a measure of the statistical accuracy of the measured intensity, being the ratio of the deviation from the average intensity to the average intensity summed over all reflections. R factors are calculated ,in LAUENORM, for reflections which are symmetrically related and should consequently have the same intensity (neglecting anomalous scatterers).

The R factors produced after the wavelength normalisation process are given in tables 2 (a),(b) and (c), along with the number of reflections in each wavelength bin. The overall R factor and the R factors as a function of resolution (produced by Rotavata/Agrovata) are tabulated for both stations in table 3.

The red crystal R factors are both very good, those from 9.5 being slightly better. The merging R factors in table 2c (for con - A) show that good data are available throughout the 0.5 - 2Å wavelength range.

5. Conclusions.

1. Station 9.5 in unfocussed mode provides a wavelength spread at high intensity of 0.2 Å to 2Å.

2. The relative exposure times between stations 9.7 and 9.5 in unfocussed mode is approximately four depending on beam horizontal steering.

3. The source horizontal position variability has been evident during the course of these experiments.

4. The Laue data quality recorded on 9.5 is at least as good as that recorded on 9.7.

Fig 1. The layout of the 9.5 hutch is shown prior to installation of the monochromator and associated slits. The cooled aperture reduces the beam allowed into the hutch from 4mrad to 3mrad by removing the innermost milliradian. This is followed by a set of adjustable slits, and an adjustable pinhole with four different apertures varying from 1.5mm to 200μm. The goniostat sits on a vertical and horizontal alignment carriage which can be moved to the back or front of the hutch.

Figs 2, 3, 4, 5 show patterns recorded from the red crystal on stations 9.5 and 9.7. Figs 2 and 3 are the "A" (or front) film from packs exposed on 9.5 and 9.7 respectively. The more intense pattern on the 9.5 photograph is the result of scaling exposure using ionisation chamber readings on separate stations on different days - the 9.5 picture (taken first) was given eight times the exposure based on previous experience of ion chamber readings on 9.7, whereas the actual reading obtained on 9.7 gave only four times the exposure (corresponding to the inverse square fall off of intensity between 9.5 and 9.7). The crystal to film distance on both stations was 60mm.

Figs 4 (9.5) and 5 (9.7) show the F (or sixth) film from the same packs giving a direct comparison of the relative intensities of the remaining short wavelength component. The dark line on the 9.5 photographs is due to the different kind of direct beam stop used.

Figs 6 and 7 show the front (or "A") films from con - A patterns recorded on 9.5 and 9.7 respectively, with a crystal to film distance of 75mm. These patterns were recorded from the same crystal during the same SRS injection. The 9.7 film is clearly stronger (in fact the "B" film was closer in intensity to the 9.5 case) due to the higher beam current and the side pole contribution. The spots on the 9.5 pattern are sharply defined, and the pattern extends with measurable intensity to the edge of the film where spots are stimulated by the longer wavelengths. Note the stronger "direct beam" mark due to the harder wavelengths present on 9.5.

Fig 8 shows the way overlap of the main wiggle and the orbit restoring wiggle contribute to the beam as seen from 9.5 and 9.7. This leads to two sources being visible on both stations, the sources being well separated on 9.5 and almost overlapping on 9.7. The main pole has (approximately) a 5T field, and the side pole 2.5T. The angles between the station and the wiggler main pole are 8mrad for 9.5 and 28mrad for 9.7. The wiggle itself has a 9mm displacement over a distance of 25cm.

Fig 9. The λ - curves (a) for the two stations have been determined from a small organic molecule (the "red" crystal). The scale of the curves is such that the highest value in each is set to unity - there is no curve to curve scaling. The Br and Ag absorption edges are clearly visible. The bias towards the harder radiation on 9.5 is shown by comparing the scale factor at longer wavelengths with that at shorter wavelengths for the same curve - the ratio is smaller for the 9.5 curve. (b) gives the curve from con - A for 9.5 only.

Table 1.

Calculated Fluxes for Stations 9.5 and 9.7 from the Wiggler Main and Side Poles.

λ[Å]	9.5 main pole	9.5 side pole	9.7 main pole	9.7 side pole
2.5	1.89×10^{10}	2.16×10^{10}	6.62×10^{10}	7.54×10^{10}
2.0	2.68×10^{10}	2.58×10^{10}	1.02×10^{11}	1.08×10^{11}
1.5	3.36×10^{10}	2.4×10^{10}	1.31×10^{11}	1.21×10^{11}
1.0	3.64×10^{10}	1.43×10^{10}	1.38×10^{11}	9.84×10^{10}
0.5	2.5×10^{10}	1.63×10^{9}	8.18×10^{10}	2.62×10^{10}

Notes -

a) Flux into a 0.1% bandwidth at the given wavelength per mrad horizontal and for a beam current of 200mA, vertically integrated into a 200μm "collimator" at the centre of the fan. .

b) Be window thicknesses included 0.75mm (9.5), 1mm (9.7).

c) The main pole ratios (9.7:9.5) are generally less than the geometrically expected factor of four because of the difference in the wiggler field strength that the two stations "see". The side pole ratios are generally greater than four due to the closer overlap on 9.7.

Table 2.

Merging R Factors as a Function of Wavelength after λ - Curve Determination in LAUENORM.

a) Red Crystal 9.5

λ Å	0.38	0.42	0.45	0.48	0.58	0.66	0.74	0.82	0.91	1.07	1.2
Bin	1	2	3	4	5	6	7	8	9	10	11
1	11.6 *47*	15.4	9.0	6.1	5.2	4.2	6.0	6.0	5.5	2.3	4.1
2	*33*	10.1 *35*	5.9	10.7	6.2	6.3	17.0	6.1	13.9	10.2	7.7
3	*42*	*37*	5.1 *44*	5.1	4.2	5.4	4.9	7.5	6.4	12.1	6.3
4	*60*	*54*	*29*	6.2 *49*	5.0	5.0	4.2	3.8	10.5	4.9	8.5
5	*58*	*80*	*138*	*161*	4.7 *244*	5.1	5.3	5.6	8.8	5.2	3.6
6	*29*	*37*	*56*	*72*	*355*	3.9 *211*	3.6	5.1	7.7	4.3	4.6
7	*19*	*18*	*27*	*42*	*148*	*294*	3.1 *200*	5.6	8.6	8.4	0.0
8	*8*	*16*	*16*	*17*	*59*	*105*	*225*	3.9 *228*	6.8	3.9	3.2
9	*6*	*4*	*5*	*4*	*16*	*39*	*59*	*97*	4.9 *56*	9.5	0.0
10	*2*	*5*	*1*	*2*	*10*	*11*	*14*	*26*	*54*	2.9 *52*	2.6
11	*4*	*2*	*1*	*4*	*7*	*5*	*0*	*4*	*0*	*26*	4.9 *22*

b) Red Crystal 9.7

λ Å	0.41	0.44	0.48	0.55	0.61	0.67	0.73	0.79	0.85	0.91	1.07	1.2
Bin	1	2	3	4	5	6	7	8	9	10	11	12
1	16.7 *8*	10.0	8.7	6.8	7.8	8.2	10.9	11.5	13.2	4.3	10.0	0.0
2	*58*	10.8 *37*	9.6	6.4	6.9	7.5	7.0	6.6	5.4	3.9	13.7	14.7
3	*61*	*74*	6.7 *11*	7.0	6.3	7.3	7.4	4.8	5.8	7.2	6.1	17.4
4	*54*	*82*	*148*	7.0 *118*	6.2	5.6	5.6	5.3	7.1	2.4	5.7	11.0
5	*38*	*44*	*84*	*235*	7.8 *133*	6.4	5.6	4.9	5.1	6.6	6.5	14.8
6	*27*	*25*	*61*	*132*	*234*	5.2 *77*	4.6	4.4	5.0	5.8	6.3	14.4
7	*18*	*19*	*33*	*70*	*136*	*238*	3.7 *99*	4.4	5.3	7.2	6.1	15.9
8	*12*	*8*	*18*	*36*	*58*	*93*	*188*	5.2 *125*	3.8	6.0	4.5	9.7
9	*8*	*8*	*11*	*20*	*34*	*46*	*74*	*152*	3.4 *72*	5.6	5.9	9.5
10	*5*	*5*	*6*	*8*	*14*	*23*	*31*	*44*	*83*	6.8 *20*	7.3	9.3
11	*3*	*6*	*6*	*10*	*11*	*12*	*19*	*22*	*37*	*55*	5.6 *51*	5.7
12	*0*	*3*	*2*	*5*	*6*	*3*	*6*	*3*	*2*	*9*	*55*	4.7 *40*

c) Con - A (9.5).

λ Å	0.6	0.7	0.8	0.91	1.06	1.17	1.29	1.4	1.52	1.64	1.75	1.86	1.98	2.1
Bin	1	2	3	4	5	6	7	8	9	10	11	12	13	14
1	17.0 *58*	15.7												
2	*86*	12.0 *106*	11.5											
3		*82*	11.6 *135*	10.5										
4			*175*	8.8 *199*	12.2									
5				*79*	9.5 *266*	8.7								
6					*200*	6.3 *369*	7.2							
7						*219*	6.9 *359*	7.2						
8							*264*	6.8 *442*	7.3	14.7				
9								*366*	8.9 *442*	7.3	2.0			
10								*2*	*290*	6.8 *306*	8.4			
11									*2*	*286*	8.5 *235*	8.1	15.0	
12											*164*	7.8 *165*	9.8	14.7
13											*1*	*148*	13.1 *101*	19.7
14												2	*116*	15.2 *73*

The merging R factors (on intensity) in percent are given in ordinary type, and the numbers of single Laue reflections contributing to each R factor are given in italics. R factors are binned as a function of wavelength. Table a) gives the R factors from the red crystal data recorded on 9.5, and b) from 9.7. Table c) gives data from 9.5 for con - A, the crystal is of higher symmetry and nearly set, therefore the symmetry related reflections span only a few bins and the matrix is nearly diagonal. Previous experience in recording λ - curves from the protein pea lectin shows that this narrow "sampling" of wavelength gives an identical curve to that produced from data where the symmetry equivalents span a larger number of bins.

Table 3.

R Factors vs resolution - Red Crystal.

	9.7		9.5	
D_{min} (Å)	R(%)	N_{meas}	R(%)	N_{meas}
1.58	5.4	83	5.2	59
1.41	5.7	174	4.3	92
1.29	5.6	154	3.9	119
1.2	5.1	234	4.7	211
1.12	5.6	256	4.6	247
1.05	5.3	232	4.6	230
1.0	7.5	200	5.2	249
Overall R	5.7 %		Overall R	4.7 %

References.

[1] R.C. Brammer, J. R. Helliwell, W. Lamb, A. Liljas, P. R. Moore, A. W. Thompson and K. A. Rathbone NIM A271 (1988) 678 - 687.

[2] J. R. Helliwell (1989) Proceedings of the 6th Joint Yugoslavian - Italian Crystallographic Conference held in Pula, May 1989.

[3] G. N. Greaves, R. Bennett, P.R. Duke, R. Holt and V. P. Suller NIM 208 (1983) 139.

[4] M. Helliwell, D. Gomez de Anderez, J. Habash, J. R. Helliwell and J. Vernon *Acta Cryst.* B45 (1989) 591.

[5] P. A. Machin Computational Aspects of Protein Crystal Data Analysis (Proceedings of the Daresbury Study Weekend) DL/SCI/R25 (1987) 75 - 89.

[6] J. R. Helliwell *J. Mol. Struct.* 130 (1986) 63.

[7] J. R. Helliwell, J. Habash, D. W. Cruickshank, M. Harding, T. J. Greenhough, J. W. Campbell, I. J. Clifton, M. Elder, P. A. Machin, M. Z. Papiz and S. Zurek *J. Appl. Cryst.* 22 (1989) 483 - 487.

[8] J. W. Campbell, J. Habash, J. R. Helliwell and K. Moffat *Inf. Quarterly on Protein Cryst.* 18 (1986) 23 - 32.

[9] S. M. Clark NIM A276 (1989) 381.

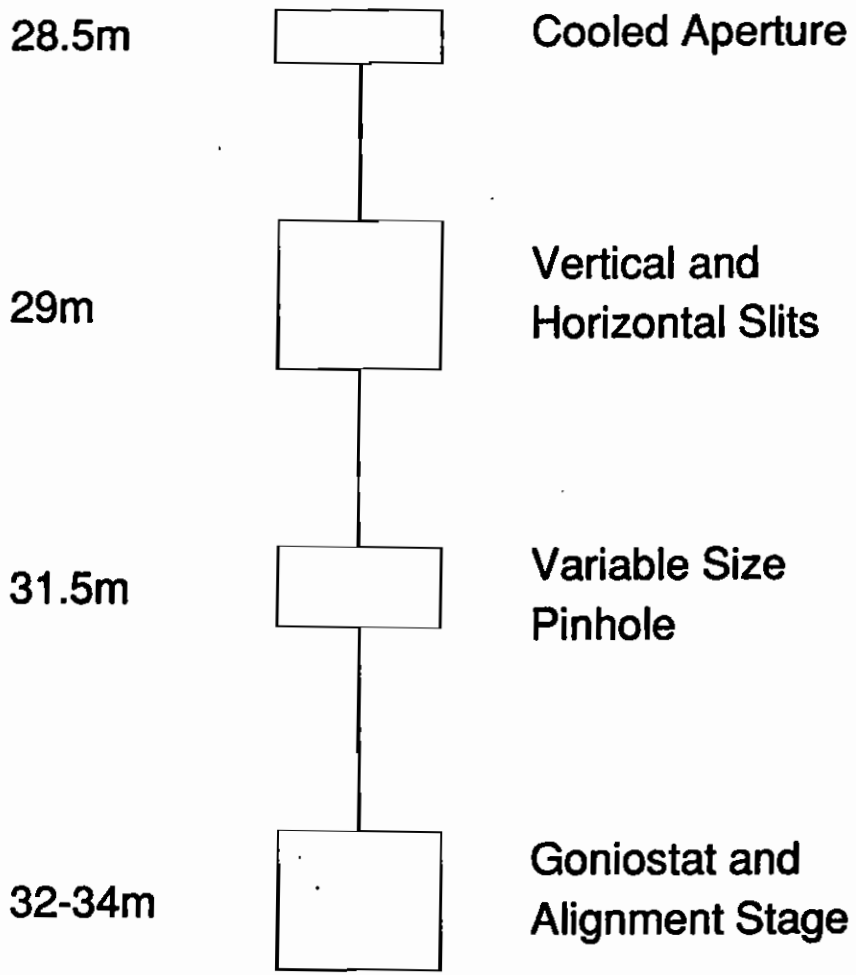
28.5m
Cooled Aperture
29m
Vertical and
Horizontal Slits
31.5m
Variable Size
Pinhole
32-34m
Goniostat and
Alignment Stage

Fig.1

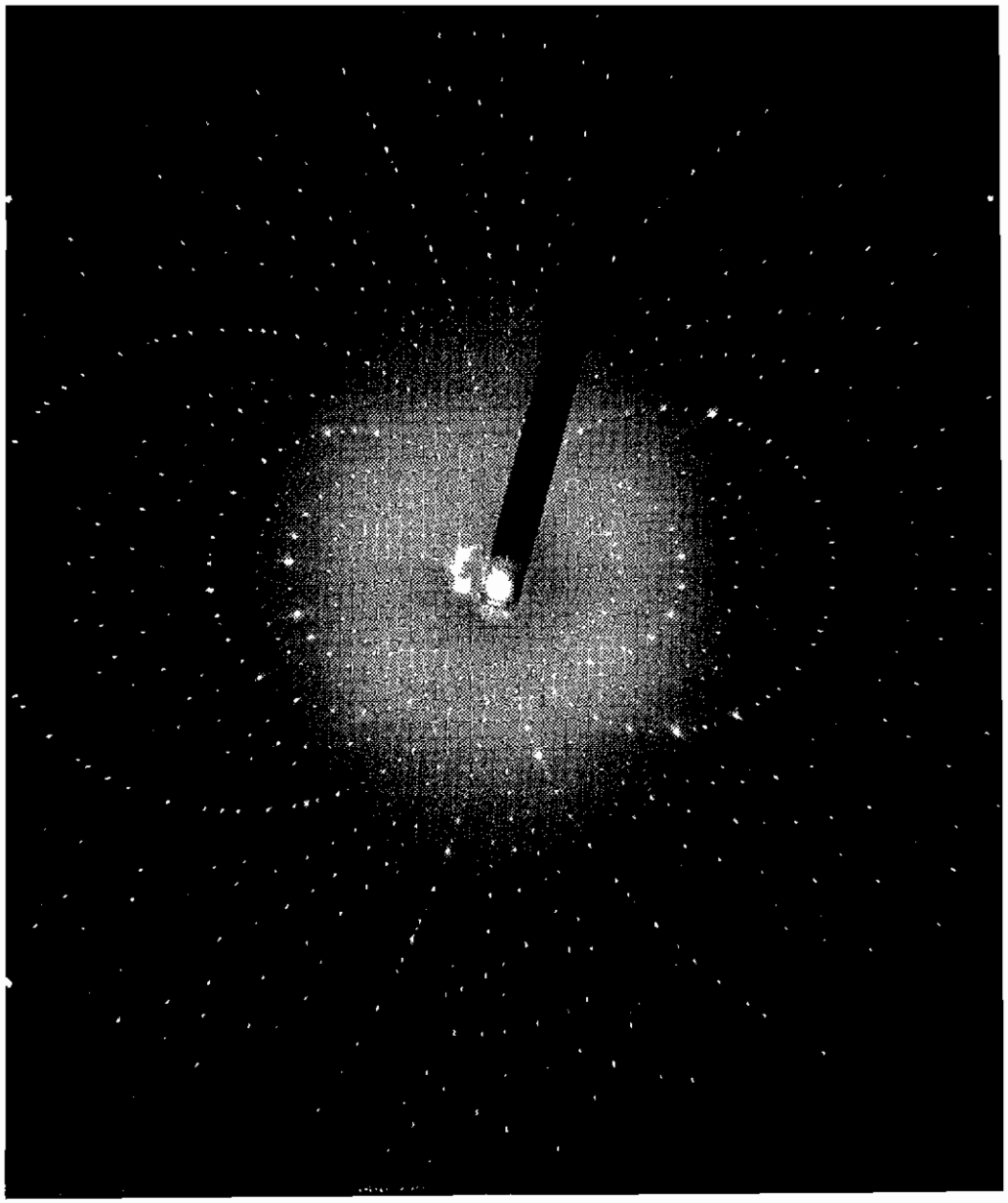

Fig.2

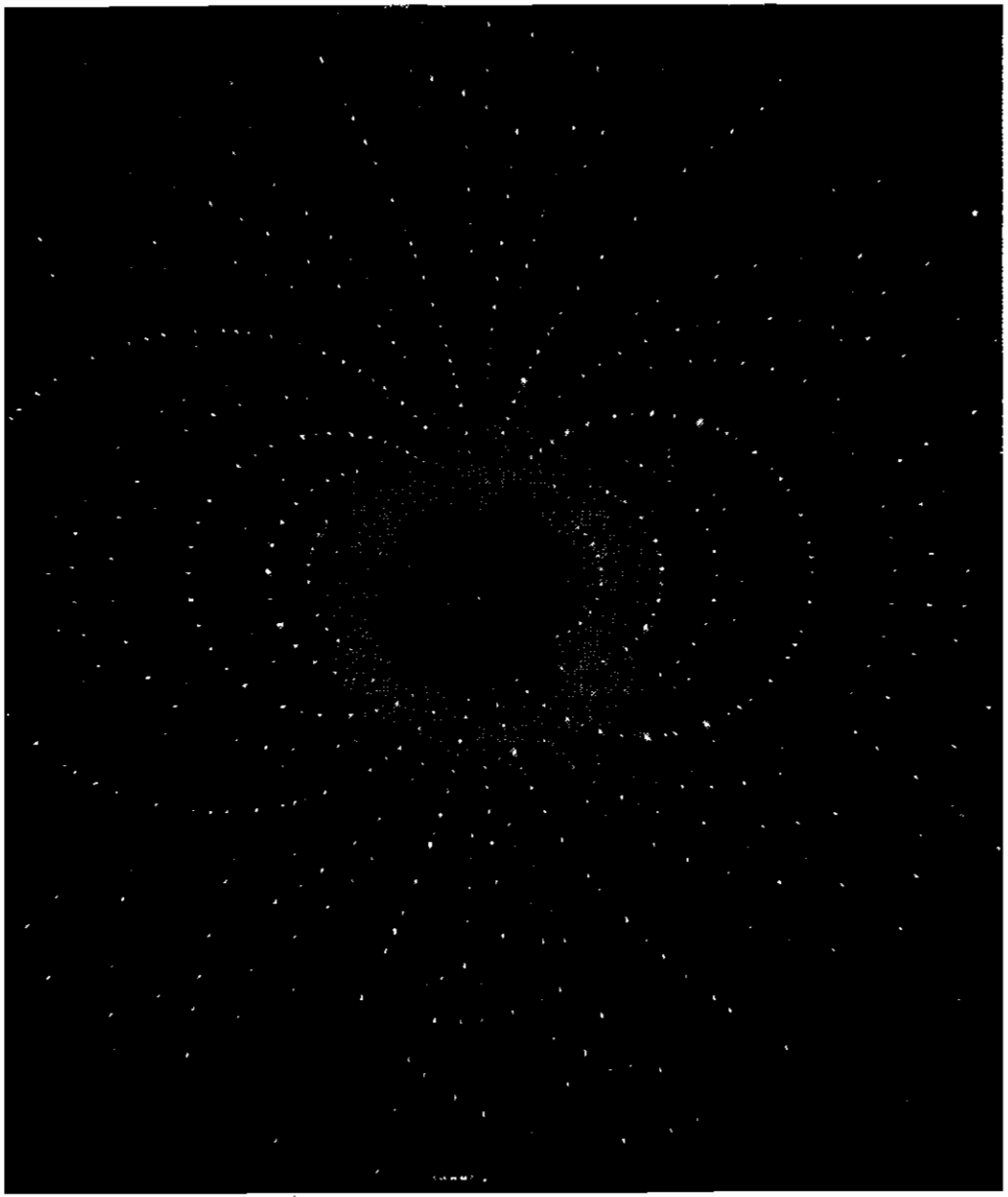

Fig.3

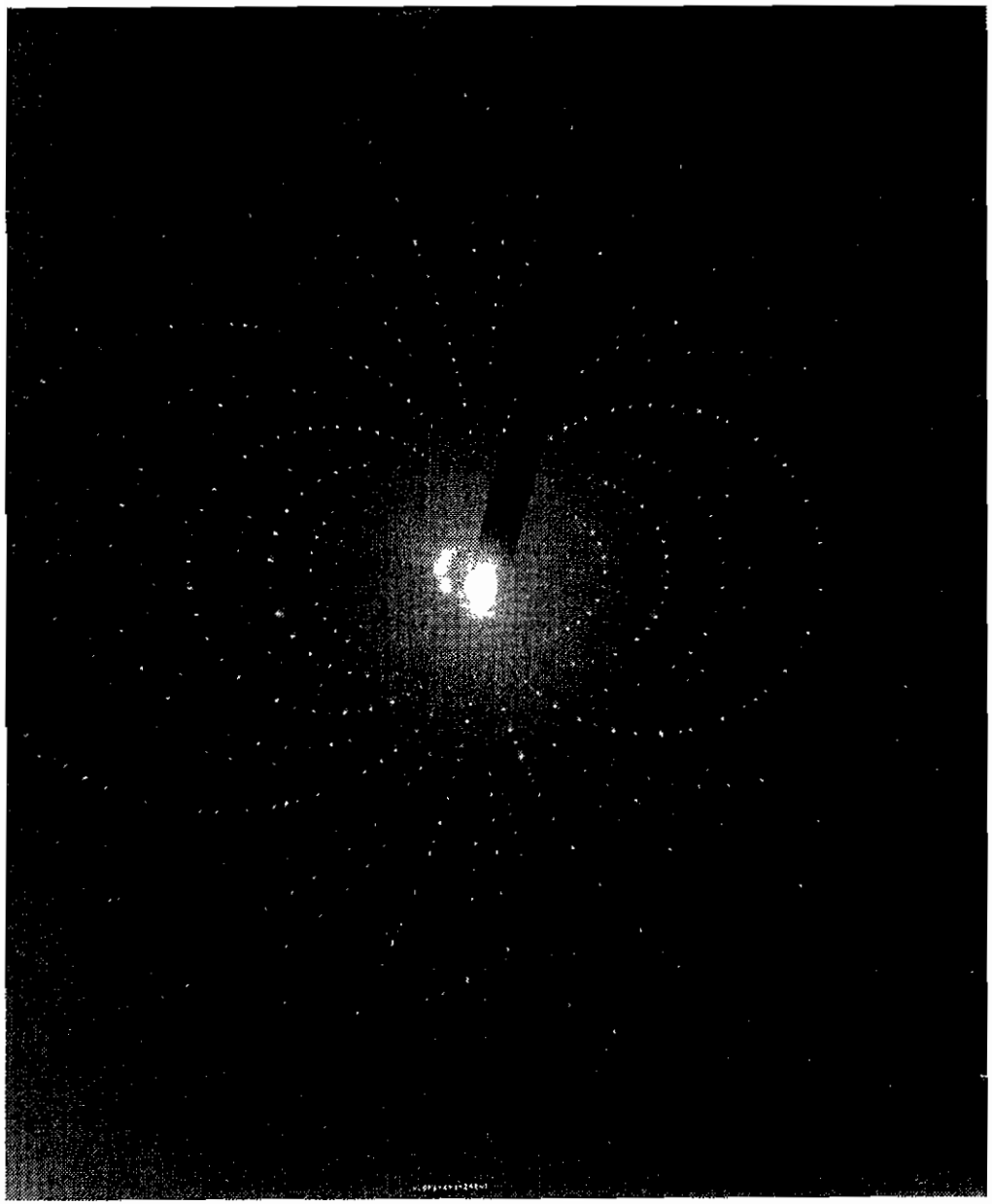

Fig.4.

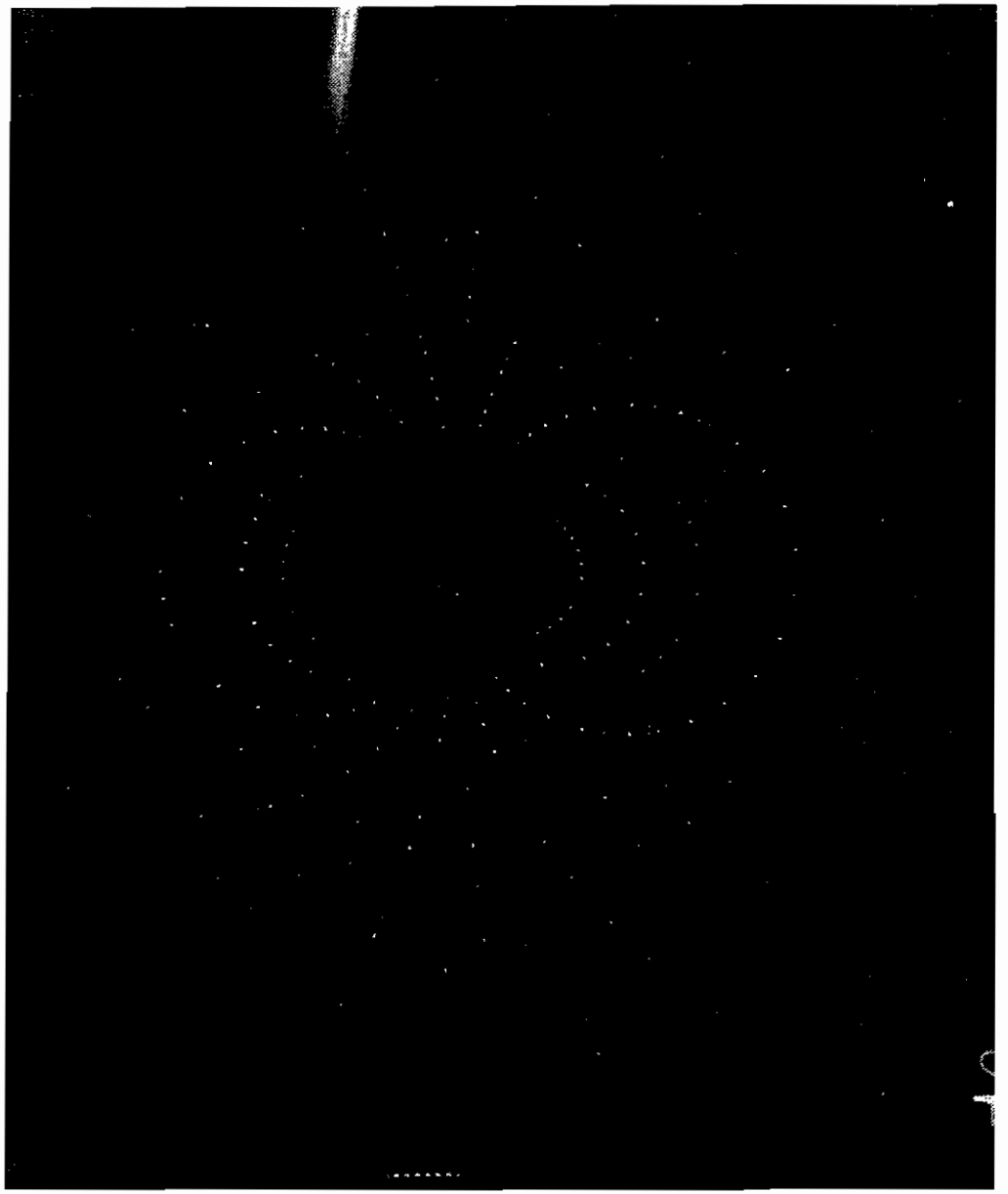

Fig.5

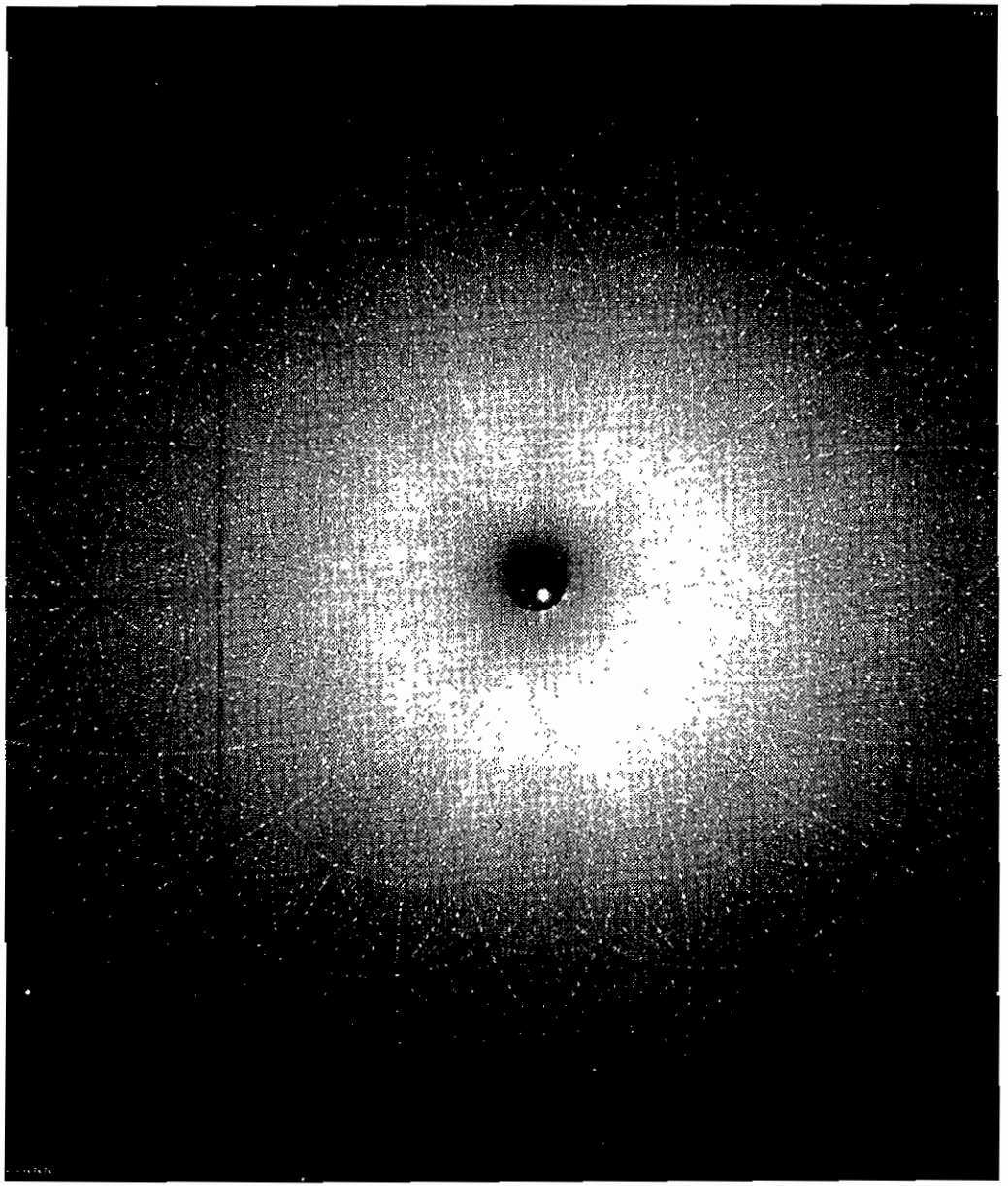

Fig.6

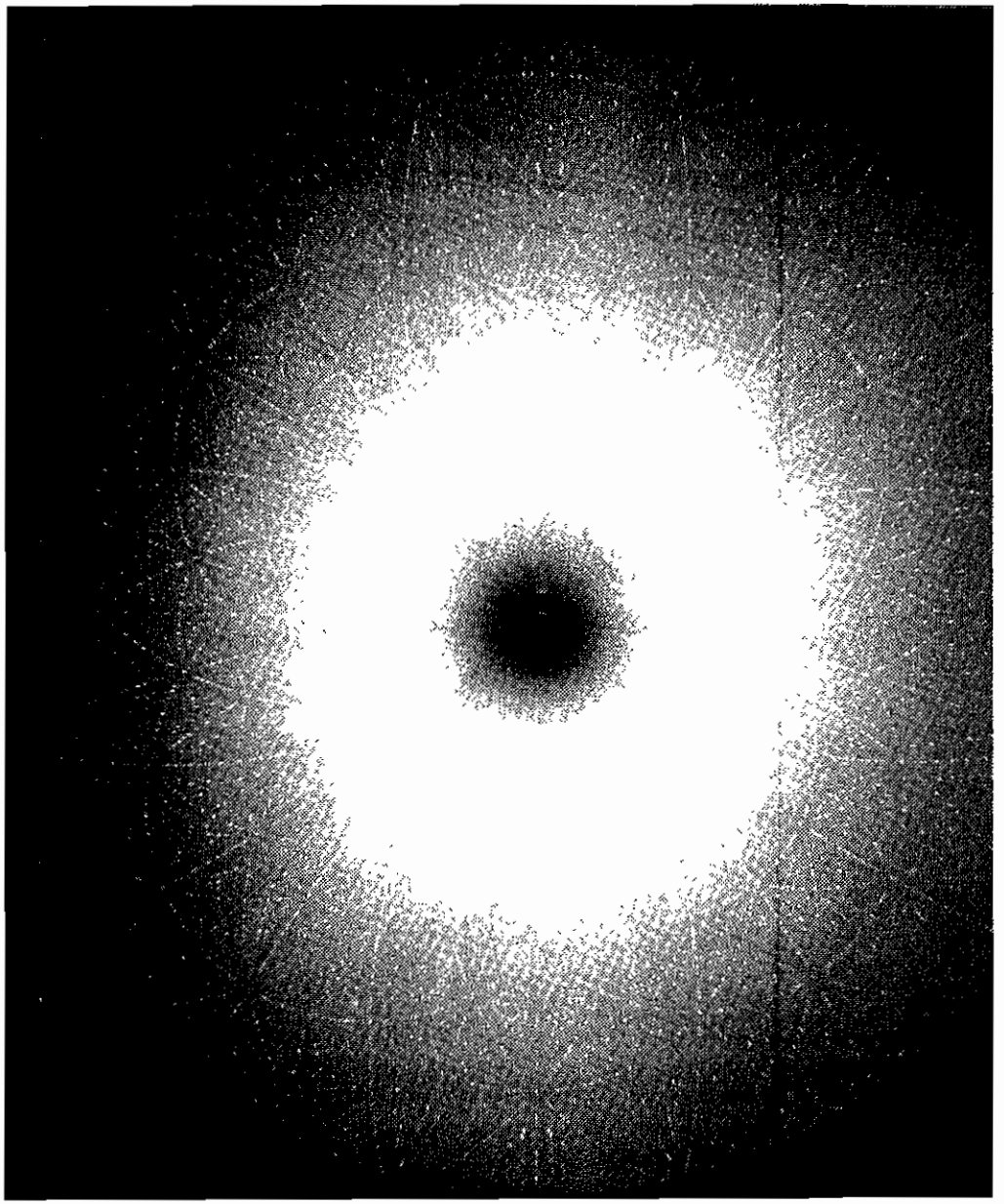

Fig.7

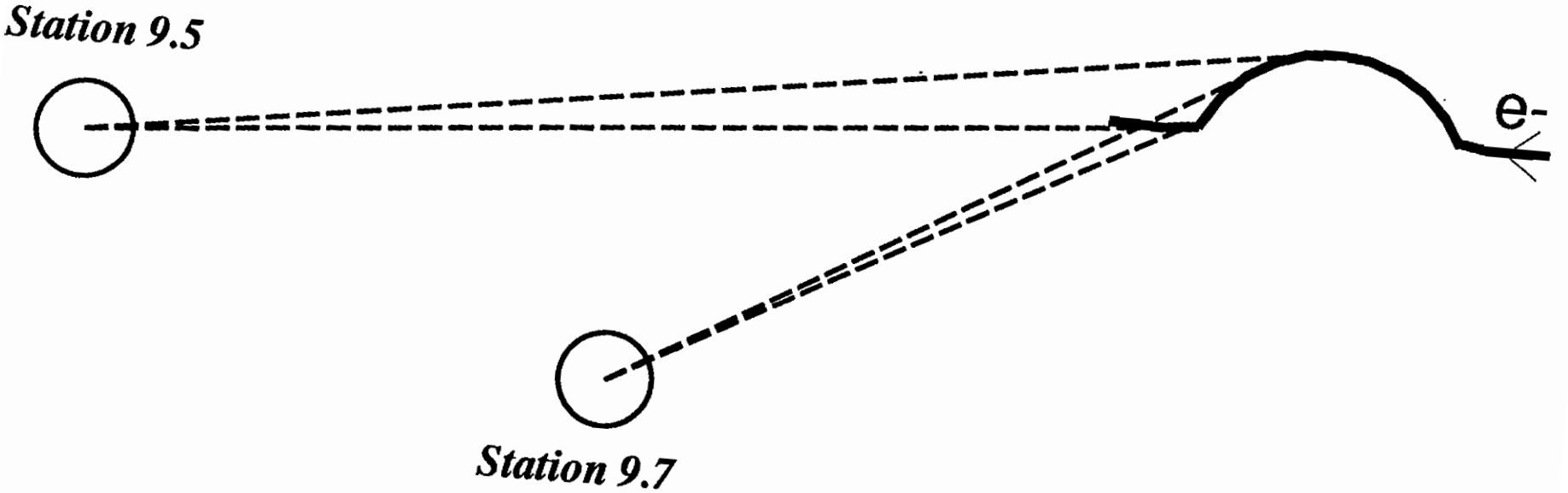

Fig.8

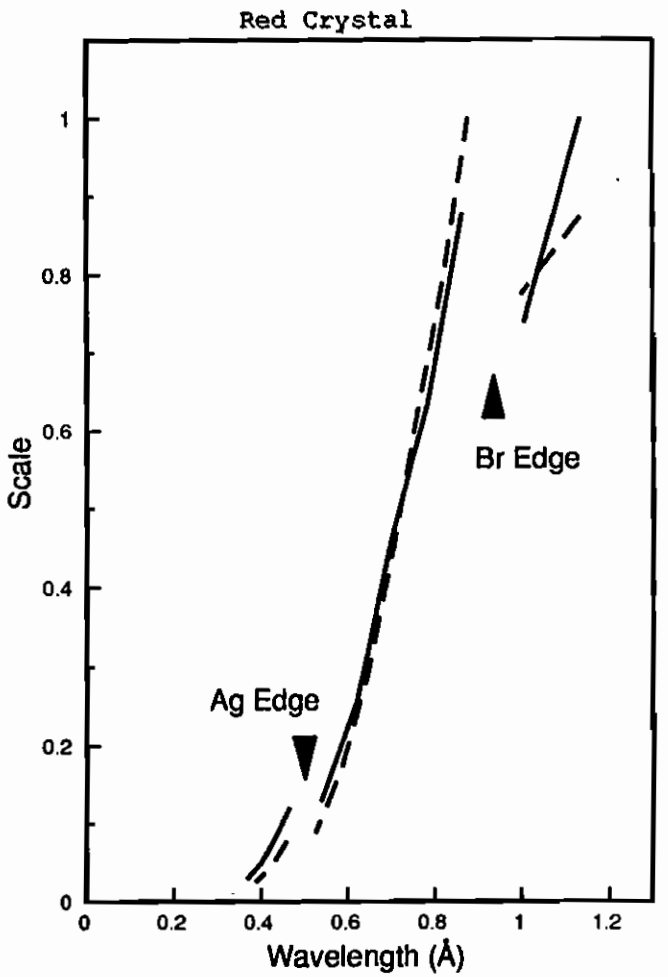
Red Crystal
Scale
Wavelength (Å)
Ag Edge
Br Edge
0
0.2
0.4
0.6
0.8
1
1.2
Solid Curve 9.5
Dotted Curve 9.7

(a)

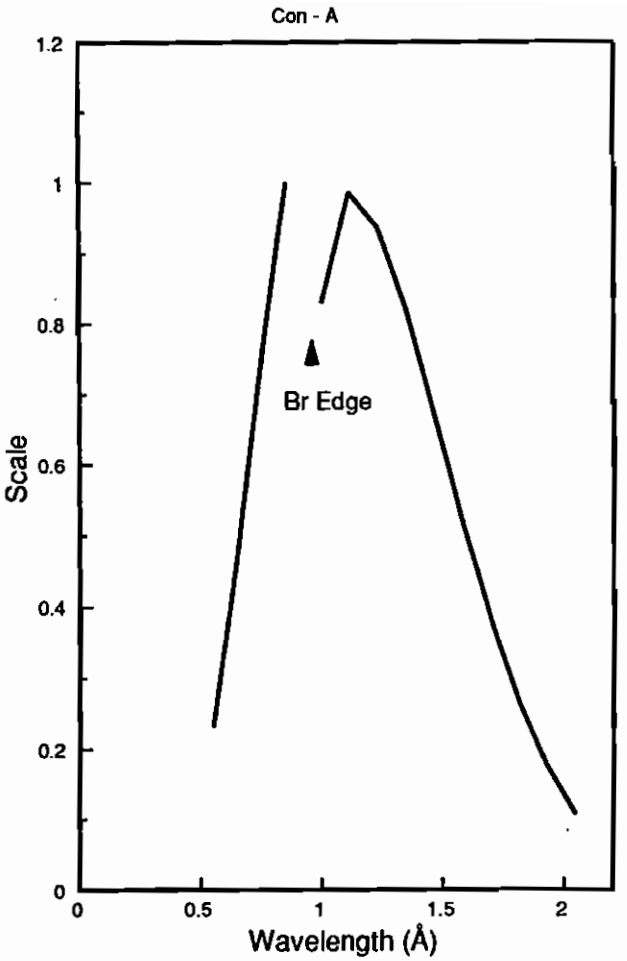
Con - A
Scale
Wavelength (Å)
Br Edge
0
0.2
0.4
0.6
0.8
1
1.2
0.5
1.5
2

(b)

Fig.9